	Btbd12 +/+	*Btbd12* +/-	*Btbd12* -/-	Total	Ratio (Btbd12$^{-/-}$/Total)	p
E 9.5	6	15	4	25	16%	0.7653
E 13.5	22	40	10	72	13%	0.2350
21 days	79	149	29	257	11%	0.0007

Supplementary Table 1: *Btbd12*$^{-/-}$ mice are born at Submendelian ratio

Viability of *Btbd12*$^{-/-}$ mice was determined by genotyping the progeny of *Btbd12*$^{+/-}$ intercrosses at different stages of development (E9.5, E13.5 and P21). Each column represents total number of embryos carrying the respective genotype. Ratio represents the number of *Btbd12*$^{-/-}$ pups divided by total number of progeny. p- value was calculated using χ^2 test.

Maternal Genotype	Paternal Genotype	Length of Mating/ weeks	Number of Litters	Number of Pups
+/-	+/-	36.9	5	38
+/-	+/-	32.6	4	27
+/-	+/-	30.7	5	37
+/-	+/-	28.9	8	60
+/-	+/-	20.3	4	28
+/-	+/-	19.6	5	36
+/-	+/-	53.9	9	65
+/-	+/-	42.1	8	62
+/-	+/-	40.3	8	59
+/-	+/-	38.9	6	37
+/-	+/-	28.0	4	29
+/-	+/-	24.2	6	43
TOTAL				**521**

Maternal Genotype	Paternal Genotype	Length of Mating/ weeks	Number of Litters	Total number of Pups
-/-	+/+	36.9	0	0
-/-	+/+	32.6	0	0
-/-	+/+	30.7	1	7
-/-	+/+	28.9	0	0
-/-	+/+	20.3	0	0
-/-	+/+	19.6	0	0
+/+	-/-	53.9	1	2
+/+	-/-	42.1	0	0
+/+	-/-	40.3	0	0
+/+	-/-	38.9	0	0
+/+	-/-	28.0	0	0
+/+	-/-	24.2	0	0
TOTAL				**9**

Supplementary Table 2: Comparison of fertility of *Btbd12*$^{-/-}$ and *Btbd12*$^{+/+}$ mice.

Cohort of heterozygous littermate intercrosses *(top) and a cohort of* homozygous animals crossed with wild-type *(bottom)* assessing for fertility.

	Human Fanconi Anaemia	*Btbd12*$^{-/-}$	*Fancd2*$^{-/-}$	*Ercc1*$^{-/-}$	*Mus81*$^{-/-}$
Chromosomal Instability	✓	✓	✓	✓	✓
Crosslinker sensitivity	✓	✓	✓	✓	✓
UV Sensitivity	×	×	×	✓	×
Infertility	✓	✓	✓	✓	×
Growth Retardation	✓	✓	✓	✓	×
Eye Abnormalities	✓	✓	✓	×	×
Skeletal Abnormalities	✓	✓	×	×	×
Peripheral Blood Abnormalities	✓	✓	×	✓	ND[1]
Glucose Intolerance	46% patients	30% prevalence	ND[1]	ND[1]	ND[1]
Hydrocephalus	✓	✓	×	×	×
Perinatal Hepatic Failure	×	×	×	✓	×
Neurodegeneration	×	×	ND[1]	✓	ND[1]

[1] ND = Not determined

Supplementary Table 3: Comparison of the phenotypic features of *Btbd12*$^{-/-}$ mice with human Fanconi Anaemia and published SSE knockout mice.

Ticks indicate that the mouse model exhibits this phenotype, crosses indicate that this phenotype is not exhibited, ND indicates not determined. For references see main text.

Oligo Name	Sequence
V0RW_18_H08_gf2	GAGACGTTCTTGCTCCTACCCCAG
LAR3_1	CACAACGGGTTCTTCTGTTAGTCC
V0RW_18_H08_gr1	GCAATGACCCAAGAAAAGAGACAG
RAF5	CACACCTCCCCCTGAACCTGAAAC
LR	ACTGATGGCGAGCTCAGACC
GSlx4f	TATGTACATACATATGTCCTG
GSlx4r	CACATTTGACAGAAGAACAACCCC
GSlx4SAr	GCTTCACTGAGTCTCTGGCATCTC
NeoF	GGTGGAGAGGCTATTCGGC
NeoR	GAACACGGCGGCATCAG
NeoP	FAM-TGGGCACAACAGACAATCGGCTG-BHQ
DotF	GCCCCAGCACCACCATT
DotR	TAGTTGGCATCCTTATGCTTCATC
DotP	FAM-CCAGCTCTCAAGTCG-BHQ

Supplementary Table 4: Sequence of Oligonucleotides

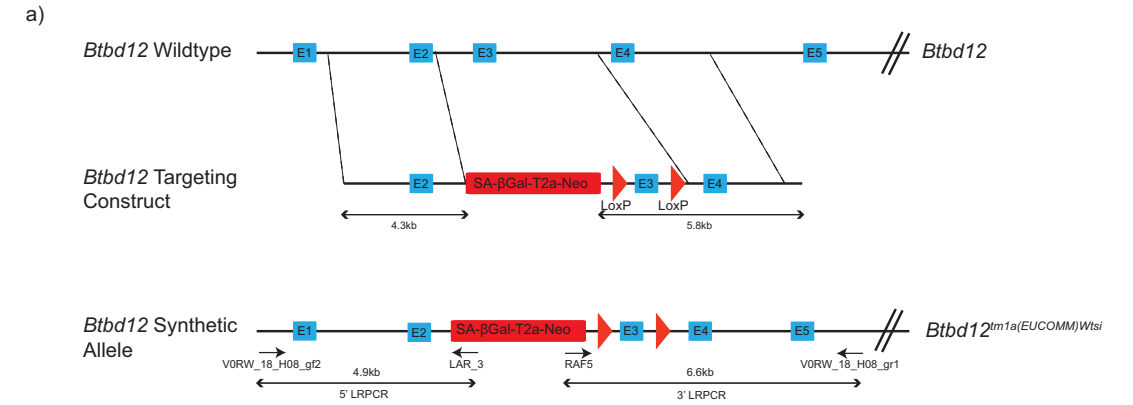

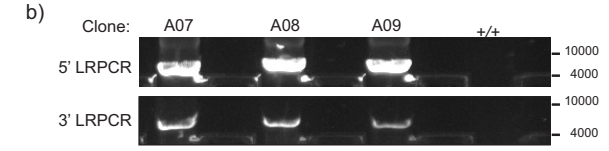

c)

	Btbd12+/+	Btbd12+/-	Btbd12-/-
Neomycin Ct	35.0000	24.5700	24.4210
DotIL Ct	22.8200	22.8400	24.6400
ΔΔCt	11.3500	0.9000	-0.1020
$2^{-\Delta\Delta Ct}$	0.0003	0.5360	1.0730
Neomycin Copy Number	**0**	**1**	**2**

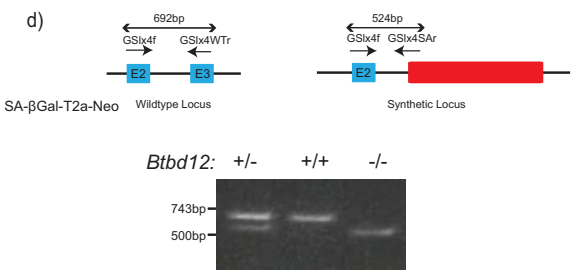

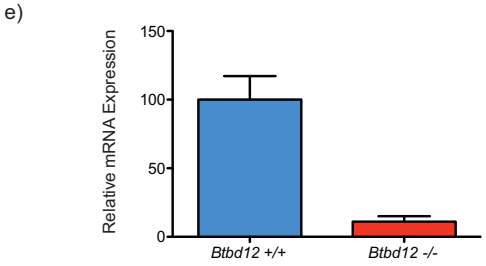

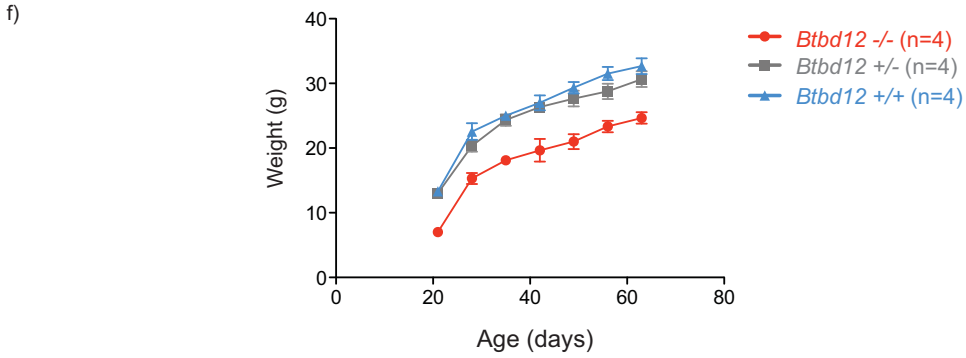

Supplementary Figure 1 Disruption of the mouse Btbd12 Locus

Supplementary Figure 1: Disruption of murine *Btbd12* locus

a) Map of the murine *Btbd12* locus illustrating exons 1 – 5. The *Btbd12* targeting construct consists of two homology arms flanking a promotorless drug resistance cassette. This cassette is constructed from a splice acceptor (SA) site followed by β-galactosidase gene (β-Gal), and finally the neomycin resistance gene (Neo). The *Btbd12* synthetic allele (*Btbd12*$^{tm1a(EUCOMM)Wtsi}$) illustrates the configuration of the locus following targeted integration of the vector. V0RW_18_H08_gf2 and LAR_3 indicate the binding sites of oligos used to determine if targeted integration had occurred using oligos 5' of the resistance cassette by long-range PCR (LRPCR). RAF5 and V0RW_18_H08_gr1 were used to confirm targeting using an oligo 3' of the integration site. **b)** Long range PCR on genomic DNA from neomycin resistant ES cell clones to determine if targeted integration of the gene-trap cassette had occurred by homologous integration. 5'LRPCR is expected to give a product of 4901bp whilst 3'LRPCR 6573bp. **c)** Neomycin copy number was determined by genomic qPCR with DNA obtained from *Btbd12*$^{+/+}$, *Btbd12*$^{+/-}$ and *Btbd12*$^{-/-}$ animals made relative to Dotl1. **d)** Map illustrating simplified *Btbd12* locus. GSlx4f and Slx4Wtr indicate the binding sites of the oligos used to amplify the wild-type locus for genotyping of mice. GSlx4f and GSlxSAr were used for PCR of the synthetic *Btbd12* locus. This confirms targeted integration as all three possible genotypes can be obtained - *Btbd12*$^{+/+}$, *Btbd12*$^{+/-}$ and *Btbd12*$^{-/-}$. **e)** Reverse Transcription qPCR analysis of the relative expression of *Btbd12* transcript in *Btbd12*$^{+/+}$ and *Btbd12*$^{-/-}$ MEFs. **f)** Growth curve of *Btbd12*$^{+/+}$, *Btbd12*$^{+/-}$ and *Btbd12*$^{-/-}$ mice (n=4, all groups; point represent mean, error bar represents standard error of mean) from weaning up to 3 months old.

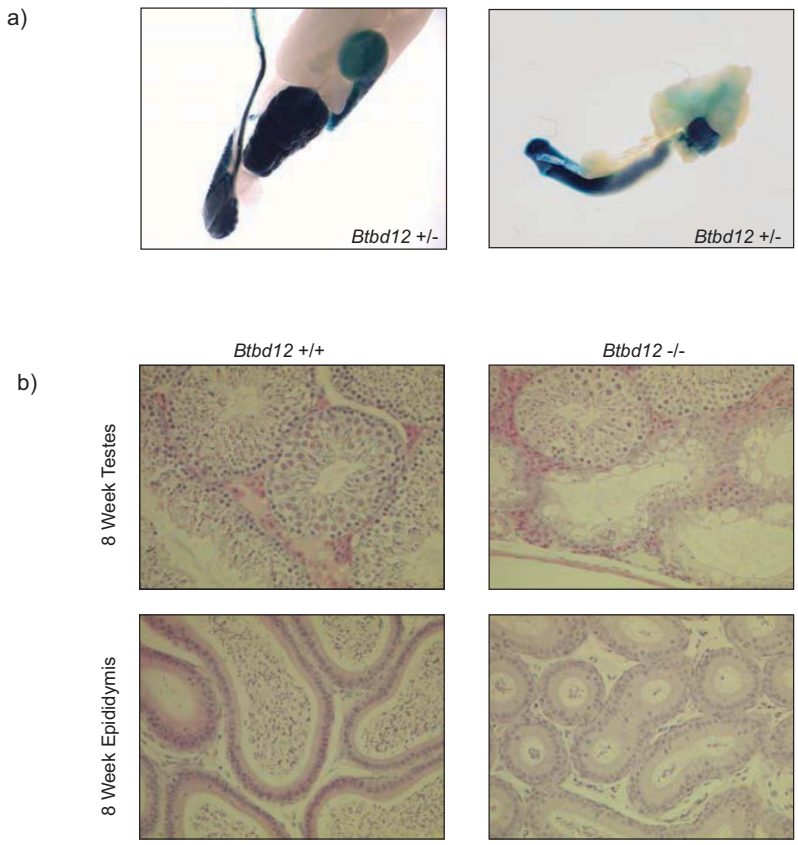

Supplementary Figure 2: *Btbd12*$^{-/-}$ reduced fertility is due to gonad failure

a) LacZ staining of testes (left) and ovary(right) from *Btbd12*$^{+/-}$ mice indicating high expression of Slx4. **c)** H&E section of testes (x400) and epididymis (x50) at 8 weeks illustrating that at 8 weeks there are fewer Sertoli-only tubules with more evidence of attempted spermatogenesis. However the epididymis of *Btbd12*$^{-/-}$ animals contains vastly reduced numbers of sperm compared with wild type littermates.

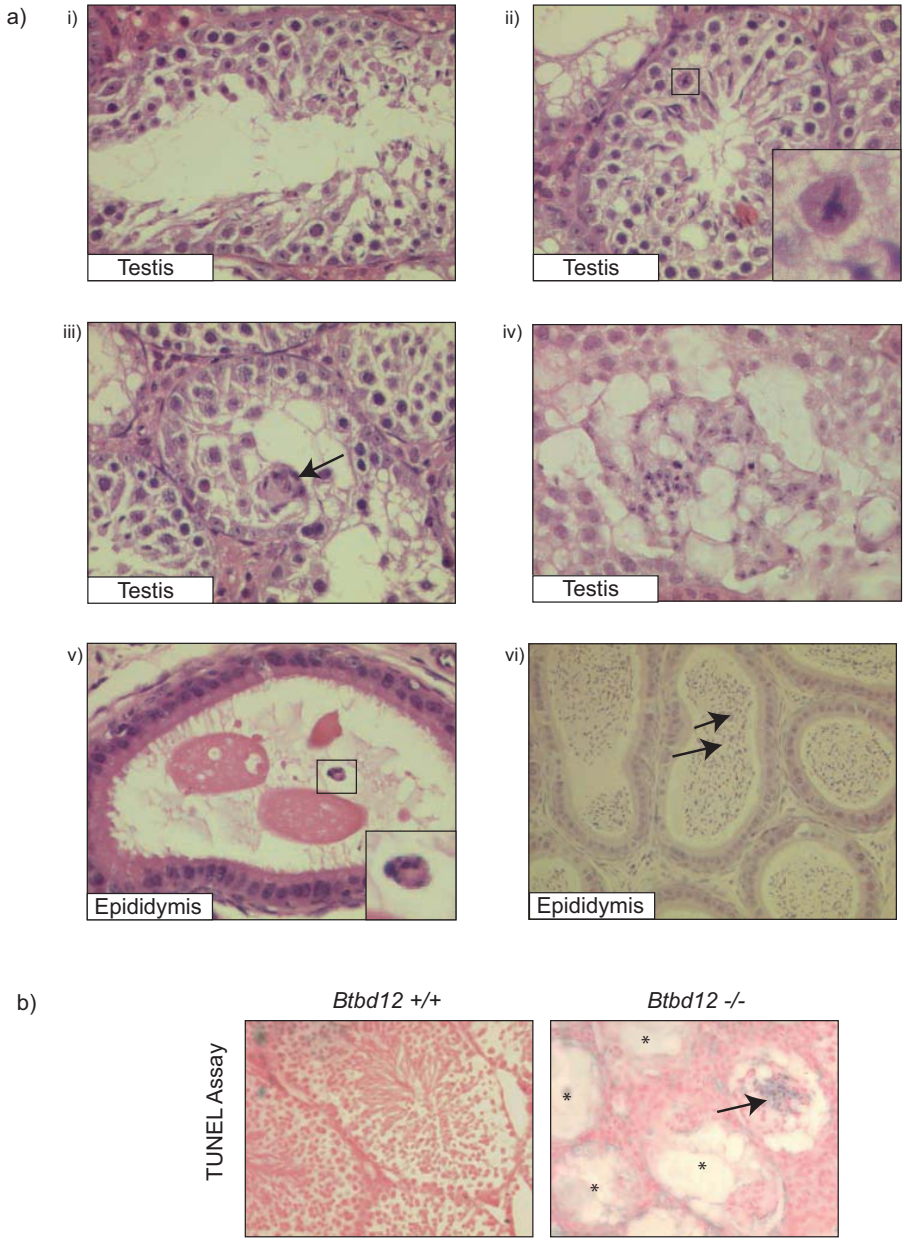

Supplementary Figure 3: Spermatogenesis is compromised with increased testicular apoptosis

a) H&E sections from gonads of *Btbd12*$^{-/-}$ mice i) The testis of an 8 week old *Btbd12*$^{-/-}$ mouse illustrating that within a single tubule spermatogenesis ranges from normal (right) to complete absence (left). ii) H&E section of testis (x400) at 8 weeks showing incomplete spermatogenesis with immature sperm being shed into lumen. Inset illustrates a dividing cell with a multipolar spindle. iii) Testis (x400) of an abnormal tubule in an 8-week-old mouse. Arrow indicates a muti-nuclear tetrad. iv) Testis (x400) of 16 week old *Btbd12*$^{-/-}$ mouse showing a tubule with a compete lack of normal spermatogenesis. All sperm being shed into the lumen of tubule are immature but at various stages of maturation. v) Epididymis (x400) for 16-week-old mouse totally devoid of sperm, inset illustrates apoptotic body. vi) A section of epididymis (x200) of 8-week-old mouse with arrows indicating large immature cells shed into the tubule. **b)** TUNEL assay, counterstained with nuclear fast red, arrow indicating increase in apoptotic cells, * indicating Sertoli-only tubules in the testis of 16-week-old *Btbd12*$^{-/-}$ mice.

a)

		Btbd12+/+	Btbd12-/-	p-value
Prevalence of Micro- or Anophthalmia		0%	36%	0.0029
Incomplete Eyelid Closure		0%	25%	0.0178
Corneal Abnormalities	**Total**	0%	72%	<0.0001
	Unilateral	0%	36%	0.0029
	Bilateral	0%	36%	0.0029
Corneal Vascularization		0%	9%	0.2619
Abnormal Iris Position		0%	36%	0.0029
Abnormal Pupil Shape		0%	27%	0.0144
Abnormal Iris Pigmentation		0%	9%	0.2619
Iris Dilation		0%	9%	0.2619
Suture Cataract		13%	20%	0.6221
Abnormal Retinal Vascularature		0%	25%	0.0378
Bergmesiter's Papilla		0%	75%	<0.0001
		n=31	*n= 11*	

b)

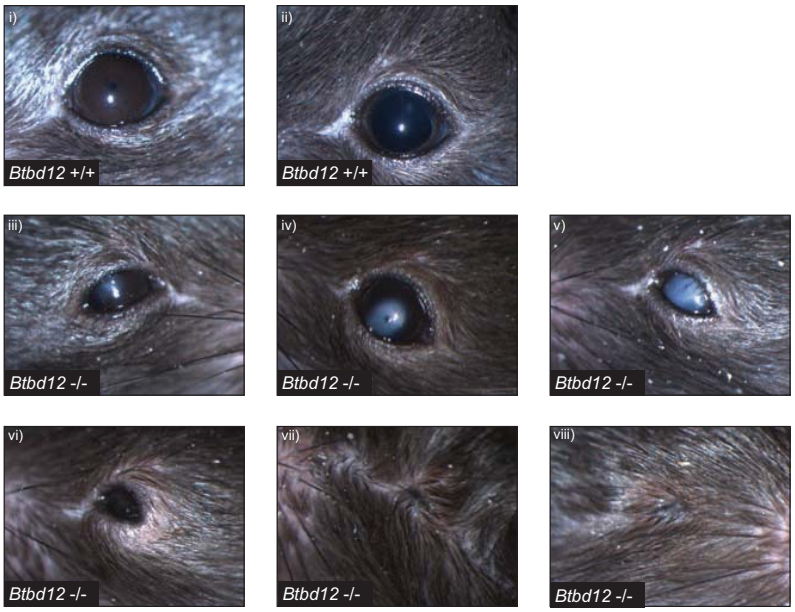

c)

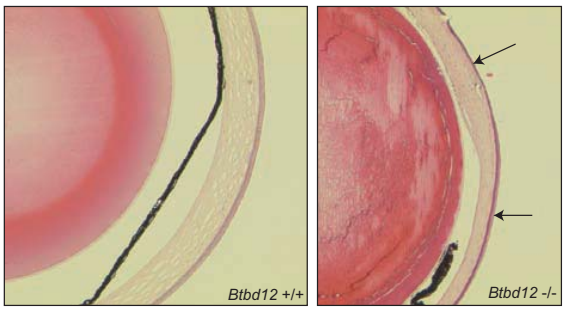

Supplementary Figure 4: Slx4 deficient mice a predisposed to a range of ocular abnormalities

a) A cohort of *Btbd12*$^{-/-}$ mice (n=11) and *Btbd12*$^{+/+}$ (n=31) were formally assessed for ocular abnormalities by slit-lamp and ophthalmoscopic examination at 13 weeks. Animals with anophthalmia, microphthalmia and corneal opacity were excluded from subsequent testing. Table indicated frequency of ocular abnormalities detected in both cohorts, p-values were calculated by Fisher's exact test. **b)** Representative Slit lamp images illustrating range of ocular abnormalities. **i)** and **ii)** wild-type mice with normal eyes. **iii)**, **iv)** and **v)** illustrate corneal opacities in these *Btbd12*$^{-/-}$ of increasing severity. **vi)** an *Btbd12*$^{-/-}$ with microphthalmia. **vii)** and **viii)** illustrate anophthalmia in *Btbd12*$^{-/-}$ mice. **c)** H&E section of *Btbd12*$^{+/+}$ and *Btbd12*$^{-/-}$ eye (x50) . Arrows indicate variation in the thickness of the corneal of the *Btbd12*$^{-/-}$ eye in an animal with corneal opacity.

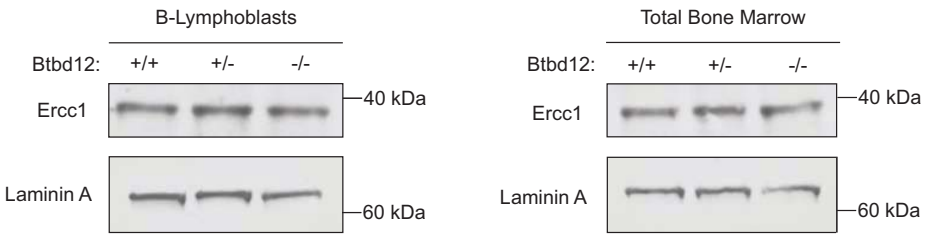

Supplementary Figure 5: Ercc1 expression is preserved in the absence Slx4 in hematopoietic compartment.

a) Ercc1 is expressed equally in LPS blasted B-lymphocytes derived from the spleen of *Btbd12*$^{+/+}$, *Btbd12*$^{+/-}$ and *Btbd12*$^{-/-}$ mice **b)** Ercc1 expression is consistent in the total bone marrow of *Btbd12*$^{-/-}$ mice, heterozygous and wild type littermates.

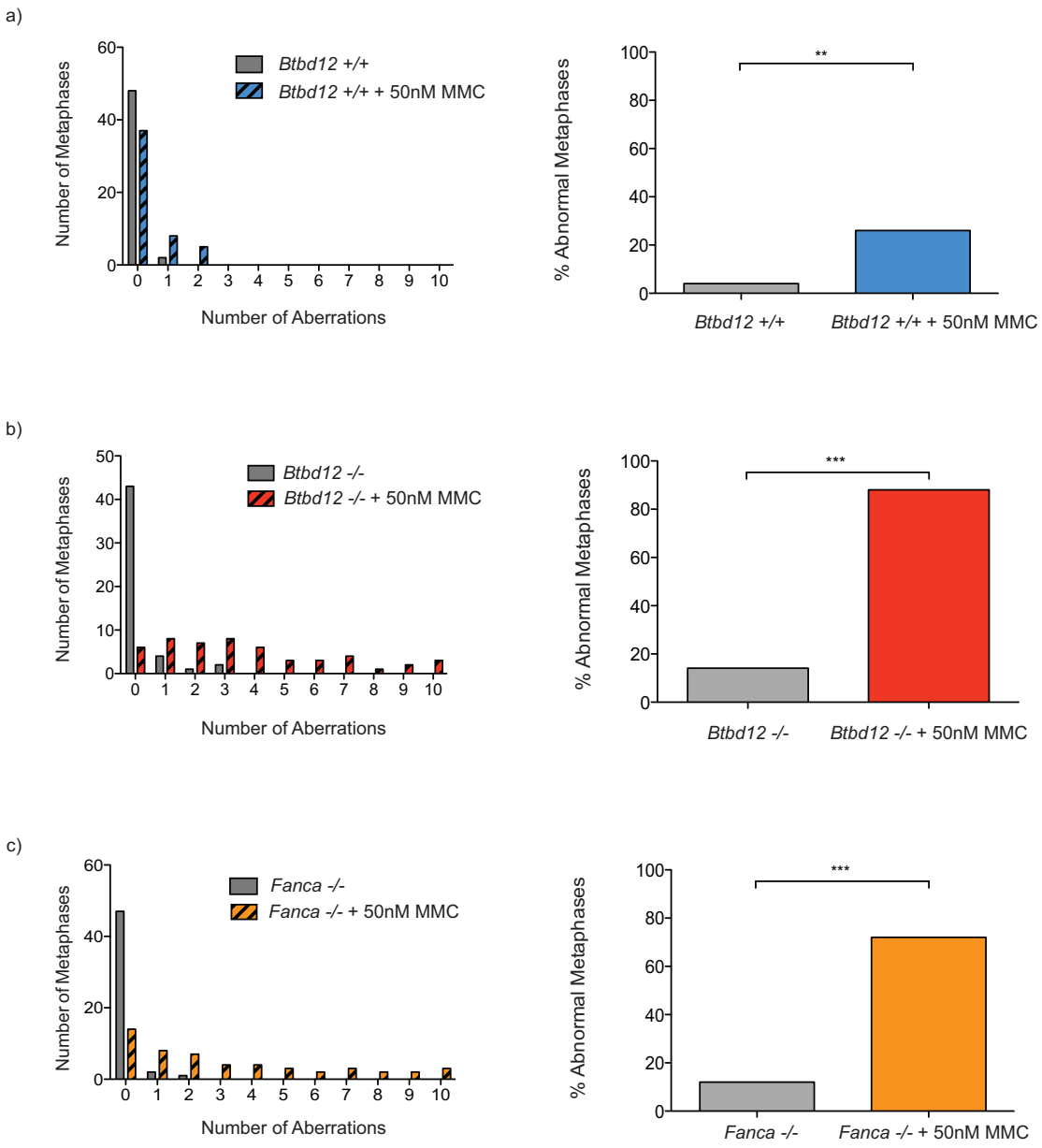

Supplementary Figure 6: *Btbd12*$^{-/-}$ and Fanca$^{-/-}$ MEFs have increased frequency of Chromosomal aberrations following DNA damage with crosslinking agent

MEFs were exposed to 50nM MMC for 48 hours and metaphases scored for aberrations. We present the number of aberrations per metaphase (left column) and the frequency of abnormal metaphases (right column) for **a)** *Btbd12*$^{+/+}$, **b)** *Btbd12*$^{-/-}$, and **c)** *Fanca*$^{-/-}$ MEFs. (**p= 0.0038, ***p<0.001 and ***p<0.001 respectively)

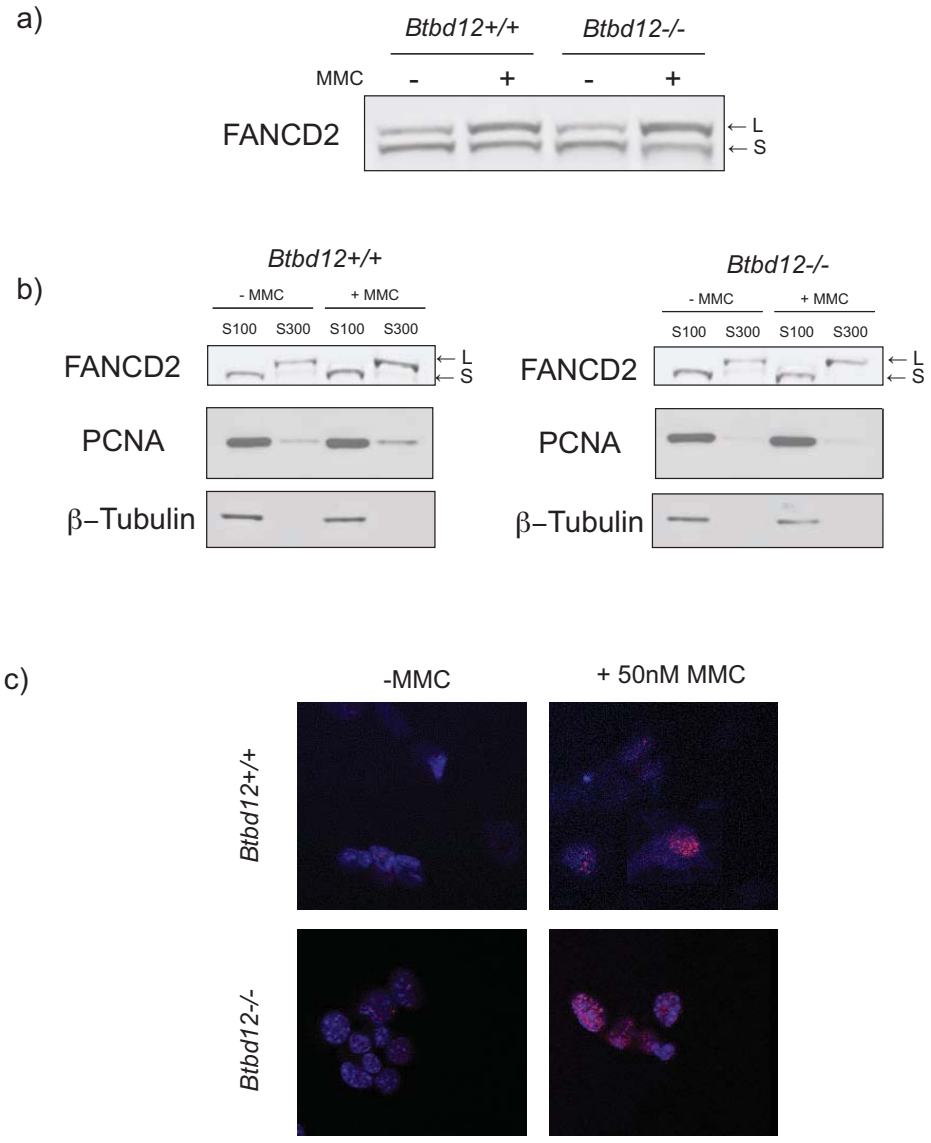

Supplementary Figure 7: *Btbd12*$^{-/-}$ cells are proficient at Fanconi Pathway activation

a) *Btbd12*$^{-/-}$ cells are competent at the monoubiquitination of FANCD2 following treatment with the DNA crosslinking agent MMC. L: Large, S: Small isoforms of FANCD2. **b)** Monoubiquitinated FANCD2 is recruited to chromatin as evidenced by its detection into the S300 fraction whilst unmodified FANCD2 is detected in the S100 fraction. **c)** FANCD2 foci formation is intact in *Btbd12*$^{-/-}$ cells following treatment with mitomycin C. Blue = DAPI, Red = FANCD2.

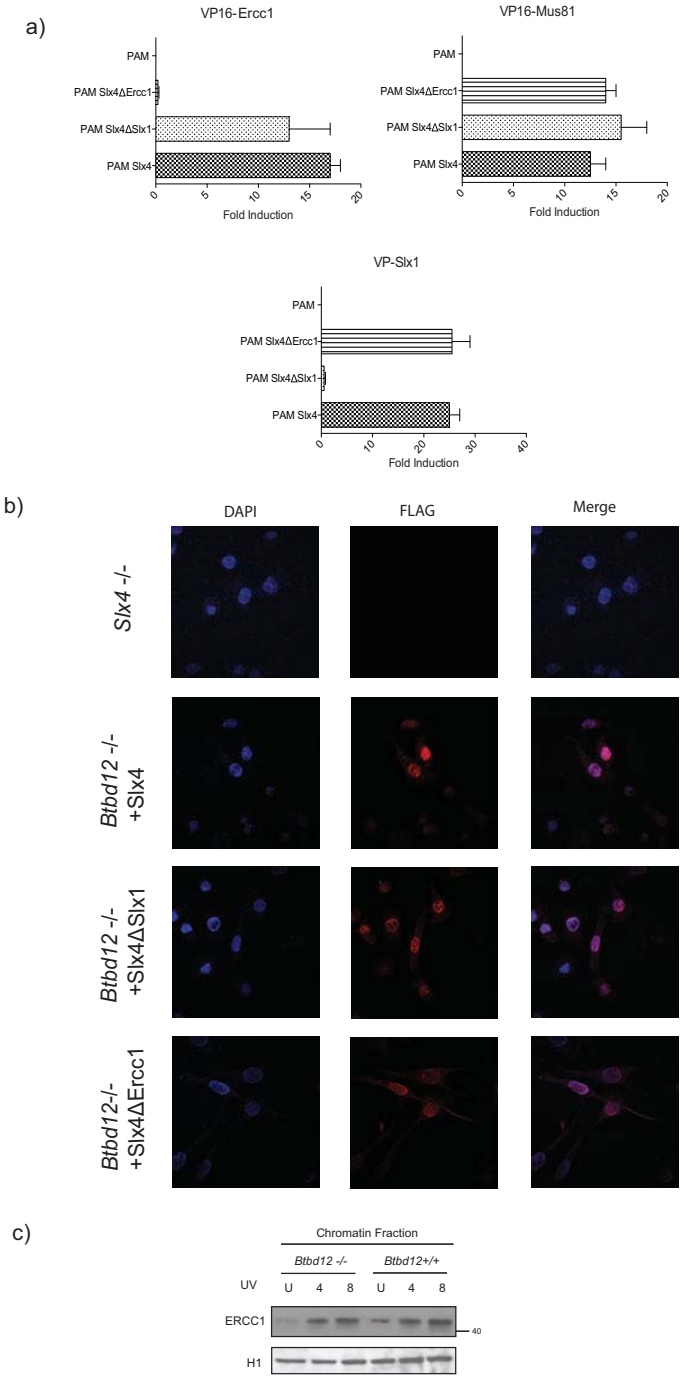

Supplementary Figure 8: Truncations of Slx4 localise to the nucleus and interact with Structure Specific Endonucleases

a) Mamalian-2-hybrid analysis of Slx4 truncations indicating that each truncation interacts with the predicted structure specific endonucleases. **b)** Truncated Slx4 proteins localise to the nucleus in *Btbd12*$^{-/-}$ cells illustrated by detection of FLAG signal in the nucleus by immunofluoresence. **c)** *Btbd12*$^{-/-}$ cells are competent in the recruitment of Ercc1 to the chromatin fraction following exposure to UV irradiation at 12 J/m^2.

a)

	Btbd12+/+	*Btbd12-/-*	p-value
Fusion of Vertebrae	33%	100%	0.0007
Processes on Vertebrae	27%	64%	0.0426
Abnormal Vertebrae Shape	0%	45%	0.0700
Abnormal Pelvis	0%	18%	0.1692
Abnormal Spine Shape	13%	100%	<0.0001
Abnormal Dentition	0%	36%	0.0221
Abnormal Skull Shape	0%	55%	0.0020
Abnormal Zygotic Bone	0%	9%	
	n=15	*n=11*	

b)

c)

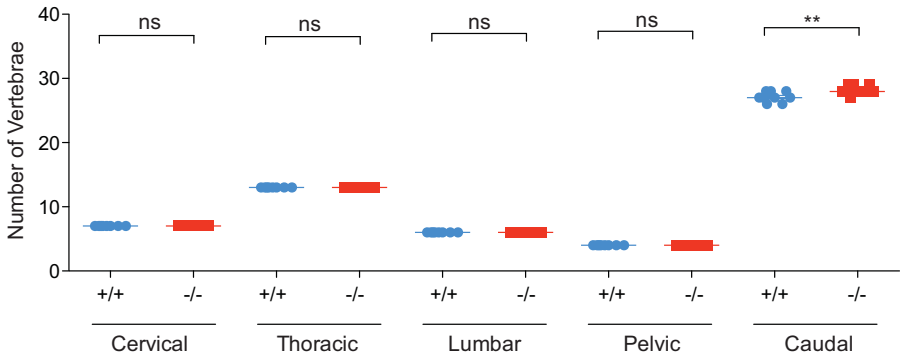

Supplementary Figure 9: Adult *Btbd12*$^{-/-}$ Mice Show a range of skeletal abnormalities

A cohort of *Btbd12*$^{+/+}$ (n=15), and *Btbd12*$^{-/-}$ (n=11) were examined using high resolution X-ray imaging at 14 weeks. **a)** Table indicating the observed frequency of a number of skeletal abnormalities. p-values were calculated by Fischer's exact test. **b)** X-ray of skull in i) wild-type, and ii) and iii) *Btbd12*$^{-/-}$ mice . Arrows indicate abnormal dentition. **d)** Vertebrae were counted in *Btbd12*$^{+/+}$ and *Btbd12*$^{-/-}$ animals and a variation was found in the number of caudal vertebrae present in *Btbd12*$^{-/-}$ mice.

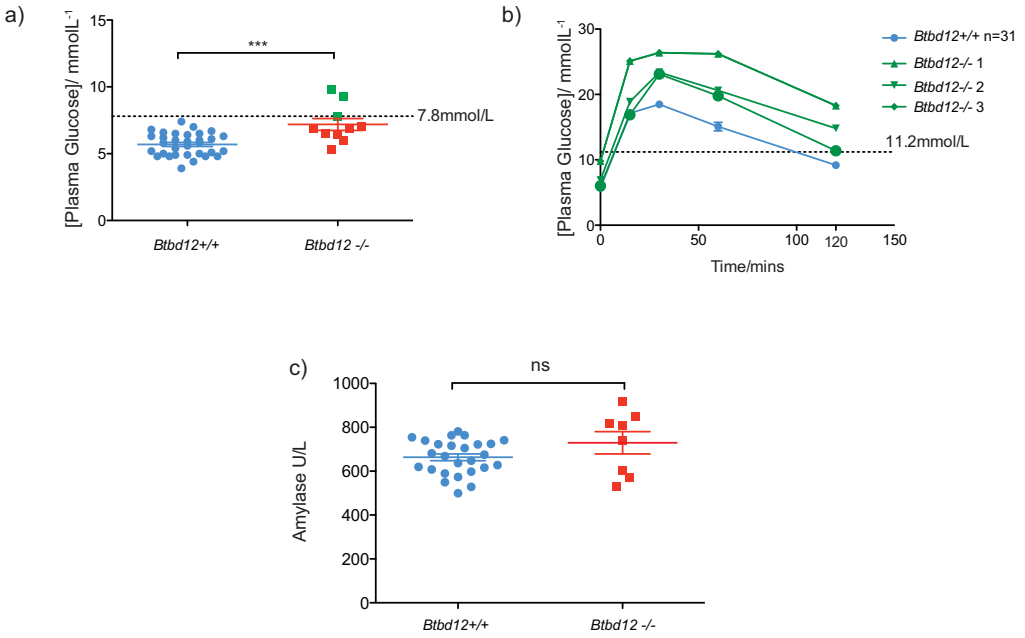

Supplementary Figure 10: Increased prevalence of glucose intolerance among *Btbd12*$^{-/-}$ mice

a) Fasting blood glucose concentration of a cohort of *Btbd12*$^{+/+}$ (n=31), and *Btbd12*$^{-/-}$ (n=10) mice. 7.8 mmol/L cut-off for normal fasting blood glucose. **b)** Intra-peritoneal Glucose tolerance testing of cohort *Btbd12*$^{+/+}$ (n=31) mice and the *Btbd12*$^{-/-}$ mice with abnormal fasting blood glucose. Three *Btbd12*$^{-/-}$ mice with abnormal fasting blood glucose also fail to return blood glucose to normal (cut-off = 11.2 mmol/L) within 120 minutes of receiving glucose challenge. **c)** Serum amylase concentration in the same cohort of mice showing no significant difference between genotypes.

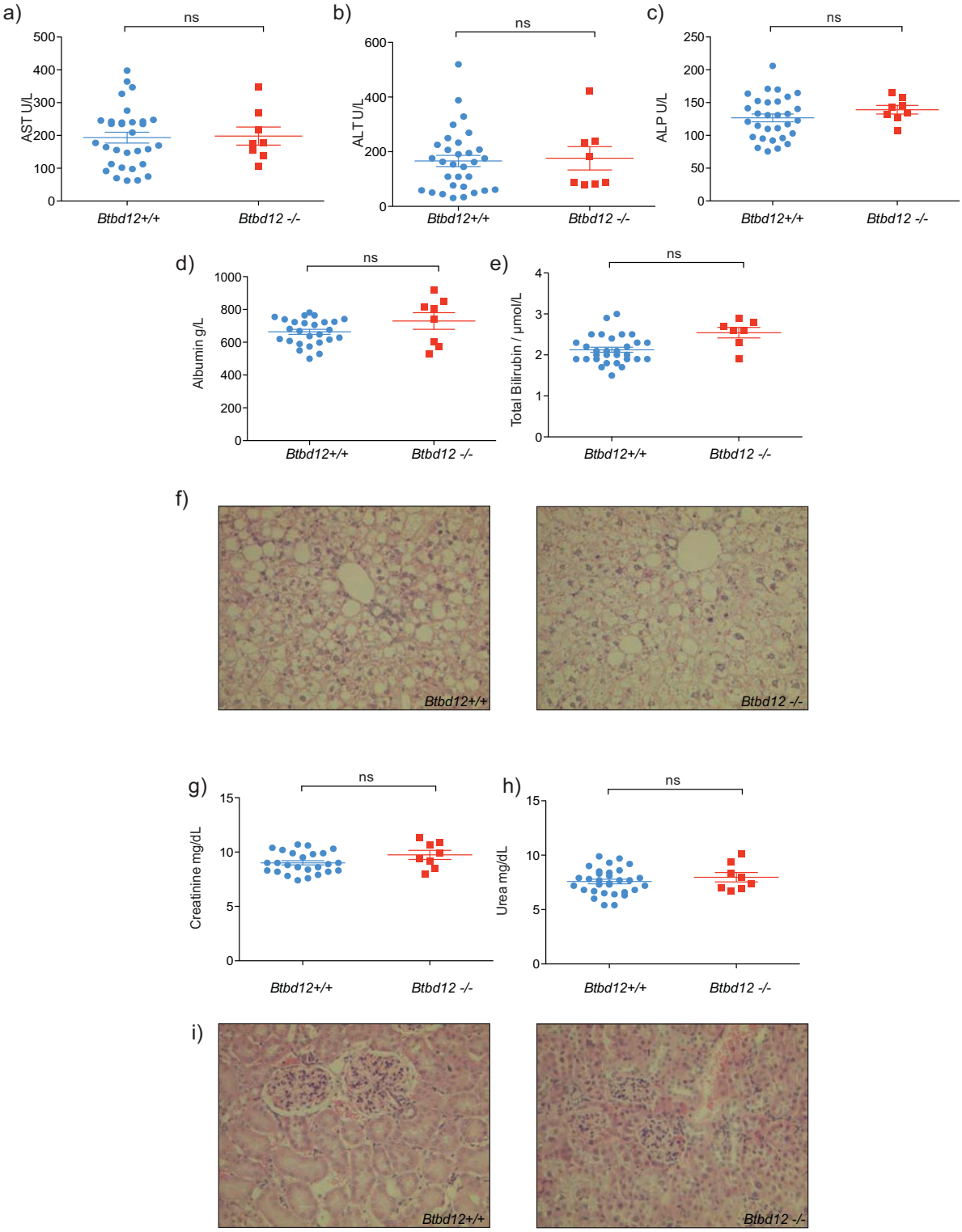

Supplementary Figure 11: *Btbd12* deficient mice do not show evidence of hepatic or renal dysfunction at 15 weeks

Btbd12 deficient mice and wild type controls were sacrificed by exsanguination at 15 weeks and serum used for clinical chemistry. No significant differences were found in the serum concentrations a panel of liver function tests; **a)** Aspartate transaminase (AST) **b)** Alanine transaminase (ALT), **c)** alkaline phosphotase (ALP), **d)** Albumin and **e)** total bilirubin. **f)** H&E section of liver (x100) did not reveal any morphological difference between *Btbd12*$^{+/+}$ and *Btbd12*$^{-/-}$ age matched animals at 16 weeks. No difference was observed in serum concentration of **g)** creatinine or **h)** urea at 15 weeks. **i)** No morphological difference was found between the kidney of *Btbd12*$^{+/+}$ and *Btbd12*$^{-/-}$ mice (H&E section x100).

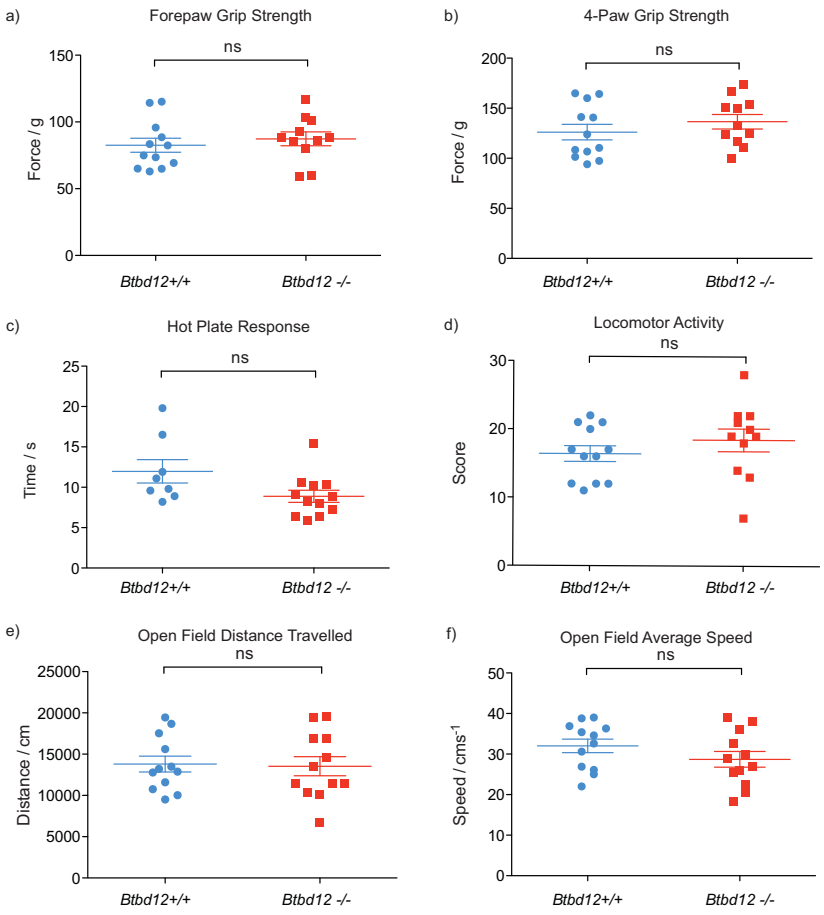

g)

Modified SHIRPA	*Btbd12+/+*	*Btbd12-/-*	p-value
Corneal Reflex	100%	100%	N/A
Contact Righting	100%	100%	N/A
Touch Escape	100%	100%	N/A
Positional Passivity	100%	100%	N/A
Pinna Touch Reflex	100%	91%	1.0000
Normal Pelvic Elevation	100%	91%	1.0000
Startle Response	100%	91%	1.0000
Normal Gait	100%	75%	0.2174
Biting Response	17%	58%	0.0894
Vocalization	17%	25%	1.0000
Tremor	0%	8%	1.0000
Trunk Curl	0%	0%	N/A
Limb Grasping	0%	0%	N/A
	n=12	n=12	

Supplementary Figure 12: *Btbd12*$^{-/-}$ are neurologically intact at 12 weeks

The neuro-behavioural and sensory status of *Btbd12*$^{-/-}$ mice was formally assessed in mice at 12 weeks. No difference was detected in the strength of either the **a)** the forepaws, or **b)** all paws. **c)** *Btbd12*$^{-/-}$ mice had a comparable response to *Btbd12*$^{+/+}$ mice when placed on a hot plate. **d), e)** and **f)** No significant differences could be found in the locomotor abilities of *Btbd12*$^{-/-}$ mice compared to wild type controls. **g)** A modified SHIRPA test was conducted on a cohort of *Btbd12*$^{-/-}$ mice and wild type littermates (n=12 per group) indicating that there is no obvious defect in *Btbd12* deficient mice. P-values were calculated using Fisher's exact test.